J Mater Sci (2006) 41:8086–8092
DOI 10.1007/s10853-006-0635-1

Electrophoretic deposition of zirconia layers for thermal barrier coatings

O. Van der Biest · E. Joos · J. Vleugels · B. Baufeld

Received: 30 March 2006 / Accepted: 30 June 2006 / Published online: 28 October 2006

Abstract This paper presents an exploratory investigation of a production route for thermal barrier coatings (TBCs) from a stable zirconia nanopowder suspension by means of electrophoretic deposition (EPD) on a low carbon steel substrate, followed by a consolidation by hybrid microwave sintering.

Since the thickness of the green deposit is restricted to a critical thickness, which depends on the curvature of the substrate, a method of repeated deposition and sintering was applied in order to produce thick coatings. The low electric conductivity of the sintered ceramic coating does not inhibit the deposition of additional layers. This method enabled the production of porous coatings with a sintered thickness of 150–300 μm.

A finite element model was applied to evaluate the thermal conductivity of the coatings. Values of the order of 0.8 W/mK were obtained which is comparable to that of coatings deposited by other techniques. Hence, the multiple deposited coatings with their thick and porous microstructure have a high potential for thermal barrier coating (TBC) applications.

Introduction

Thermal barrier coatings (TBCs) are widely applied on gas turbine parts in order to reduce the temperature of the metallic turbine blades [1–3]. Thermal barrier coating (TBC) systems exhibit different failure modes depending on the thermal and mechanical load. Some critical issues are related with oxidation deteriorating the adherence, others with interface imperfections, which amplify under cyclic thermal loading [4]. Furthermore, in service sintering of the ceramic may decrease the performance of the coating [5]. In addition to these TBC system related processes increasingly more attention is directed towards external factors like foreign object damage [6, 7] and molten sand penetrating and damaging the ceramic [8].

A number of technologies are used with plasma spraying in the case of stationary gas turbines and electron beam physical vapour deposition (EB-PVD) in the case of aircraft turbines being the most common methods although other techniques such as MOCVD are also being investigated [3, 9–13]. While these techniques are applied with great success, they are cost and time intensive and coating of complex shapes may be difficult or even impossible. As a cheaper and faster coating procedure leading to coatings, the use of electrophoretic deposition (EPD) for obtaining such layers will be investigated in this paper. EPD is indeed a very suitable method to deposit a coating on a conductive substrate [14, 15] and the coating of complex shapes is possible.

The loose powder coating needs to be consolidated after EPD, yet the high temperatures necessary for sintering with conventional furnaces may be detrimental for the metal. In this work, microwave heating has been selected since with this method, the surface of the part reaches the highest temperature, which should be high enough to consolidate the powder coating, whereas the interior of the substrate remains relatively cool.

In this exploratory study, zirconia has been selected for the TBCs and plain low carbon steel for the

O. Van der Biest · E. Joos · J. Vleugels · B. Baufeld (✉)
Department of Metallurgy and Materials Engineering, Katholieke Universiteit Leuven, Kasteelpark Arenberg 44, Leuven, Belgium
e-mail: bernd.baufeld@mtm.kuleuven.be

substrate. Clearly, the latter can only be seen as a model for the bond coated nickel based alloy used in turbines. However, since the method is quick and potentially inexpensive, it could be used for TBCs in other applications.

Experimental methods

A partially stabilised zirconia powder has been used (3 mol% Y_2O_3 stabilised grade HSY-3U from Daiichi, Japan, with a crystal size of 30 nm and specific surface of 4–10 m^2/g) with cobalt as a sintering aid (UMICORE Belgium, extra fine grade, >99.87% cobalt with a crystal size of 1.3 μm). The substrate is an ARMCO steel (pure iron, $C < 0.008$ wt%) in the form of cylinders (diameter 14.5 mm, length 20 mm) terminated on one end by a spherical cap with a height of 5 mm (see Fig. 1). The surface roughness due to machining was measured by a Taylor–Hobson profilometer to be $R_a = 1.33$ μm and $R_t = 6.72$ μm.

Approximately 50 g of zirconia powder and 0.5 g of cobalt powder in 100 ml ethanol together with 300 g zirconia balls (Tosoh, TZ-3Y) in a polyethylene container of 250 ml were mixed in a multidirectional mixer (Turbula type) for 24 h. After mixing, the powders were dried in a rotating evaporator. Suspensions with a powder concentration of 10 g per 100 ml were prepared by dispersing the mixed powders in a solvent containing 85 vol% of methyl ethyl ketone (MEK), 15 vol% of *n*-butylamine (*n*-BA) and 0.2 wt% nitrocellulose with respect to the powder mass. Prior to their use, the suspensions were first mechanically stirred for 45 min and then ultrasonically stirred for 30 min to further break-up the agglomerates. The Zeta potential of zirconia (assuming agglomerates with a radius of 0.1 μm) in this solvent was determined at room temperature to be –49 mV.

The EPD cell consisted of the cylindrical substrate which was placed in the centre of a larger stainless steel tube electrode with a diameter of 40 mm. During the EPD experiment, the steel substrate was dipped in the stirred suspension for a predefined time. After anodic EPD the coated steel cylinders were dried in air.

The green specimens were sintered at different temperatures and times in a microwave furnace in a flowing nitrogen atmosphere (L' AIR LIQUIDE Grade N28 99.997%) with a flow rate of 20 l/h. The microwave furnace used in this work was designed and fabricated by MEAC (Cera Lab II). The sample configuration in the microwave cavity is schematically shown in Fig. 2. Since the ceramic does not couple with the microwave at low temperatures a hybrid technique with a cylindrical SiC tube was applied as a susceptor.

Fig. 1 Steel substrate covered by single crack-free EPD coating

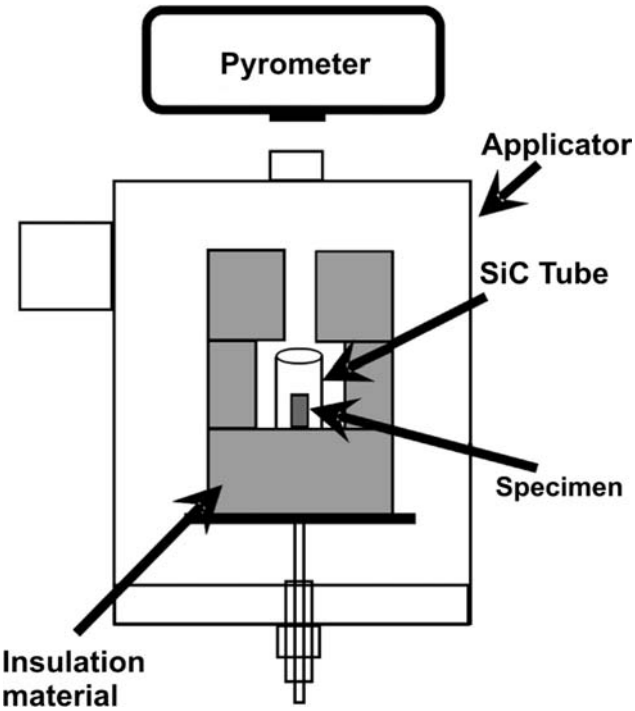

Fig. 2 Configuration of sample and SiC susceptor in the microwave applicator cavity

This susceptor homogenises the microwave field, but still allows fast heating and cooling rates [16]. The microwave oven consists of a 2.45 GHz microwave generator with a power output continuously adjustable from 0 to 2 kW, a cylindrical single-mode tuneable applicator, and a computer control system. Temperature measurements were performed with a two-colour pyrometer, positioned on top of the microwave-sintering furnace and directly focussed on the sample top surface (see Fig. 2). The working range of the pyrometer is between 700 and 2000 °C.

The density of the green coating was measured based on the Archimedes principle in ethanol (Sartorius Balance). Microstructural investigation of polished cross-section samples was performed by means of scanning electron microscopy (SEM, XL30-FEG, FEI, Eindhoven, The Netherlands). Quantitative analysis of the local chemical composition was carried out on the polished cross sections in an electron microprobe (JEOL733).

Results and discussion

Processing of single layers

Figure 1 shows the steel substrate after EPD. It is observed that a critical coating thickness exists beyond which the coating shows cracks after drying. This critical coating thickness depends on the shape of the substrate. For the geometry as shown in Fig. 1 the critical thickness was estimated at 45 μm. This thickness was calculated from the mass deposited, the green density of about 2.3 g/cm^3 (37% of the theoretical density), independently measured by means of the Archimedes principle, and assuming a uniform thickness of the coating. The cracks always originate at the transition between the cylindrical and hemispherical surfaces where its curvature is highest. If the hemispherical end is covered by a Teflon cap, the critical green coating thickness is increased to 80 μm. The mechanics of the cracking of such brittle thin films has been discussed by Hu et al. [17]. Measurement of the stresses in drying thin film has been reported by Guo et al. [18]. While the influence of humidity on the critical coating thickness was not investigated in detail, it was observed that different drying rates obtained by different temperatures does not have any apparent impact on it.

Crack free green coatings were obtained by deposition at 130 V (electric field at the substrate 177 V/cm) for about 12 s. Total deposited mass was about 100 mg. These were sintered in the microwave cavity using a heating rate of 150 °C/min, a dwell time of 30 min at the highest (sintering) temperature and a cooling rate of 50 °C/min. Figure 3 shows cross-sections of coatings sintered at different temperatures. Table 1 shows the level of porosity determined on the micrographs. With increasing sintering temperature the level of porosity decreases. Also the distribution of the pores evolves as the sintering temperature increases. At the higher

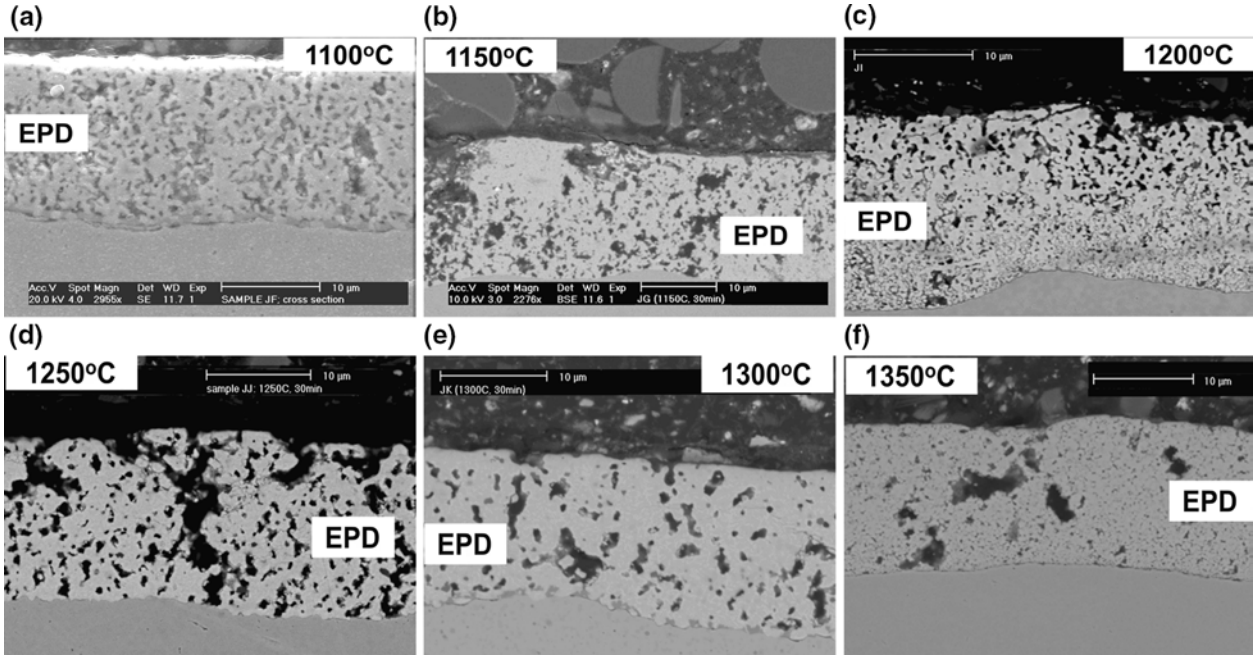

Fig. 3 Microstructure of EPD coatings sintered for 30 min at the indicated sintering temperature (substrate at the bottom)

Table 1. Porosity of the EPD coatings sintered at the indicated temperature for 30 min

Sinter temperature (°C)	1100	1150	1200	1250	1300	1350
Porosity (%)	28.7	29.4	26.9	27.6	23.2	22.4

sintering temperatures, pores appear to agglomerate so that the number of larger pores increases relative to the number of smaller ones. The pores in the coating sintered at 1350 °C appear to have a bimodal distribution, with a high number of very small pores with a few hundred nanometre diameter and a smaller number of pores with a size of 5 μm. It is clear that during sintering the substrate has exerted a constraint on the densifying coating since a plain zirconia sample can be sintered to full density at 1350 °C. However, this constraint is believed not to lead to substantial residual stresses within the EPD coating since such stresses most probably are relieved due to the high porosity and possibly by micro-cracking.

As the coating densifies and shrinks, we have obtained evidence that a thin liquid metallic layer forms underneath and penetrates the porous coating. Figure 4 shows the result of sintering temperatures higher than it was the case of the other specimens reported in this paper. In this extreme case, the liquid metal has exuded through the pores in the coating. For the coatings shown in Fig. 3, the average iron content was measured by a scanning electron beam which travelled through the thickness of the coating in steps of 1 μm. According to EDX measurements, the coating sintered at 1100 °C for 30 min has an iron content of 3.54 wt% with a standard deviation of 0.37 wt%. For a coating sintered at 1350 °C the mean value was slightly higher at 3.78 wt% with a standard deviation of 0.62 wt%. It is interesting to note, that no gradient of iron through the thickness was observed.

Fig. 4 Over-sintered EPD coating on a steel substrate showing the penetration of a liquid metal layer through the pores of the zirconia coating. This effect was not observed for the conditions reported in this paper

Processing of multiple layers

The thickness after sintering of a single layer is about 30 μm. This is insufficient for the use of TBCs, since for an effective temperature reduction the TBCs usually applied to stationary gas turbines and aircraft turbines have a thickness of at least 100 μm. The possibility to repeat several times the procedure of EPD followed by microwave sintering has been investigated. It should be mentioned that the total time taken to deposit one layer is of the order of 90 min, since EPD takes only a few seconds and the microwave cycle is of the order of 1 h. It was found that the EPD process was not influenced by the prior deposition of sintered zirconia coatings. Table 2 gives the relevant data for the EPD process in the case of multiple layers. It was noticed that the thickness of the multi-layers was no longer uniform. Possibly this was due to variations in electrical conductivity of the prior coatings. Figure 5a shows the microstructure of sintered multilayers, which were all sintered at 1200 °C for 10 min. The mean iron content in this multilayer was 1.87 wt% with a standard deviation of 0.94 wt%. Also in this case a gradient in iron concentration was not detected.

Evaluation of the thermal barrier properties

Following literature reports [19–22], the thermal barrier performance of deposited coatings was evaluated with the help of object oriented finite element analysis OOF [23] on the basis of its microstructure in cross

Table 2. EPD data for a 11-fold coating/sintering procedure (EPD voltage 130 V) on the same specimen shown in Fig. 5

	Mass deposited (mg)	Time (s)	Current (mA)
EPD 1	93	9	76
EPD 2	107	10	72
EPD 3	144	9	34
EPD 4	111	10	102
EPD 5	129	8	26
EPD 6	170	15	66
EPD 7	173	13	19
EPD 8	125	12	47
EPD 9	129	17	36
EPD 10	104	12	21
EPD 11	159	13	16
Total	1444		

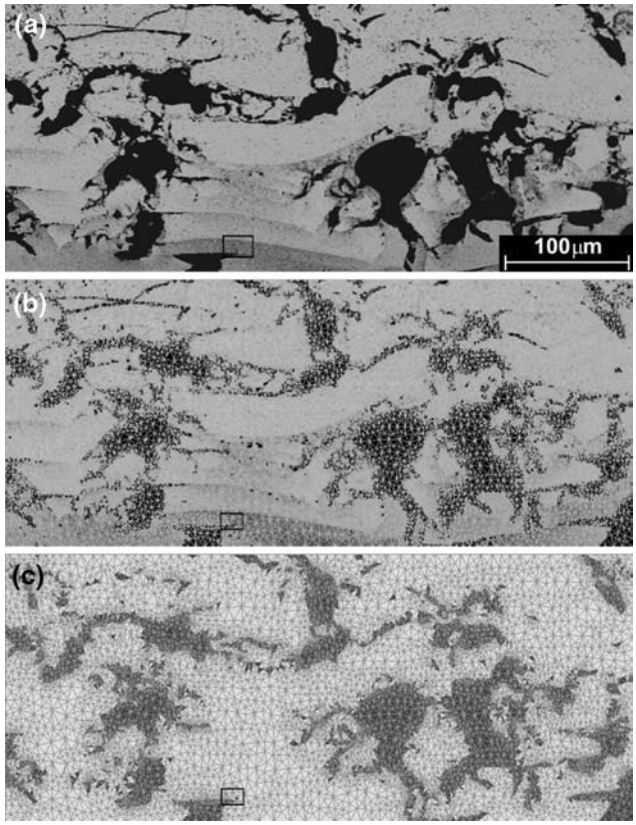

Fig. 5 (**a**) Microstructure of a EPD coating resulted from 11 repeated EPD procedures (see Table 2) and microwave sintered after each deposition step at 1200°C for 10 min. The image of the substrate on top has been removed. (**b**) The same image after selection of the phases and creation of a mesh. (**c**) The mesh after assignment of one phase to each element. The box indicates a region shown in detail in Fig. 6

section. This property is characterised by the effective thermal conductivity, which should be a value between the thermal conductivity of air which fills the pores and that of completely dense zirconia. The OOF method starts with the preparation of the micrographs followed by the execution of the virtual experiments. The calculations were done for a micrograph of a multilayer coating prepared by 11 repeated EPD procedures. The image of the substrate, initially on top of the picture, was removed so that only the thermal barrier layer can be seen and will be evaluated (Fig. 5). Using algorithms available in the OOF program, areas belonging to zirconia and those belonging to a pore need to be distinguished. Therefore, a mesh needs to be generated which covers the microstructure so that each element contains only one phase. The fineness of the mesh is a compromise between calculation time and accuracy. Figure 5 shows the original microstructure (a), the initial mesh (b) and the mesh in which a phase is assigned to each element. The level of porosity of the sintered coating in Fig. 5 is 28.9%. This percentage is mainly due to the large pores and underestimates the true porosity since the very fine pores cannot be resolved at the magnification used. For instance, a high magnification image of the boxed area (Fig. 6) shows that it contains 27.6% fine pores, which are not included in the meshing selected.

In order to determine the effective thermal conductivity, the OOF program can calculate the temperature drop over the coating when a heat flux is imposed or vice versa the heat flux can be calculated for a given temperature gradient. In either case, the effective thermal conductivity k_{eff} can be calculated from the formula:

$$k_{\text{eff}} = \frac{q}{(T_H - T_i)/\Delta y},$$

with q the heat flux per unit area; T_H the temperature at the coating surface; T_i the temperature at the coating substrate interface; Δy the thickness of the coating. Both approaches were used in our simulation. For the case of an imposed heat flux of 1000 W/m^2 with T_H = 1600 °C, the average T_{i} was calculated to be 1085 °C. This yields an effective thermal conductivity of 0.837 W/mK. If the surface temperature is set at 1600 °C and that at the interface at 1200 °C, a heat flux of 795 W/m^2 is calculated, yielding an effective thermal conductivity of 0.855 W/mK.

The experimental results of thermal conductivity of TBCs vary very much and depend on factors like deposition technique, porosity and thermal history. The thermal conductivity of a TBC produced by EB-PVD at room temperature generally is between 1 and 2 W/mK increasing with TBC thickness and thermal

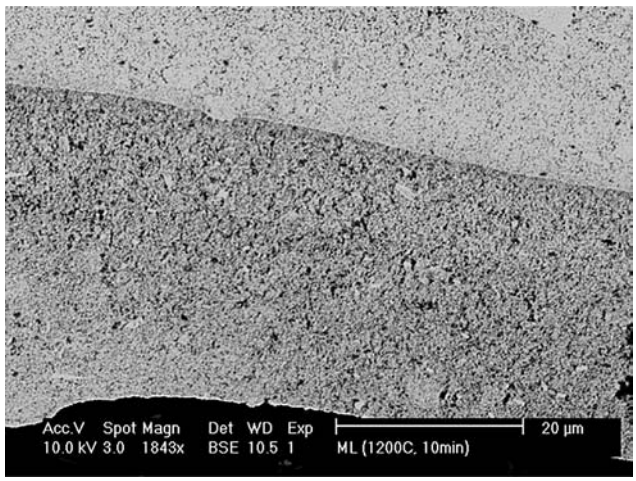

Fig. 6 Higher magnification of region indicated by the box in Fig. 5

loading [24–26]. For plasma sprayed TBCs lower thermal conductivities with about 0.8 W/mK are reported [22, 25], and agree with the present OOF results for the EPD coating. Experimental measurements of the thermal conductivity of EPD coatings are planned. Yet, due to the high porosity of EPD coatings compared even to plasma sprayed TBCs lower values than for the presently available TBC types are expected.

The OOF simulation is only an approximation of the thermal barrier capacity of the coating. Some factors which would enhance the barrier capacity were neglected such as the fine porosity and the temperature dependence of the thermal conductivity of zirconia. Other factors which increase the thermal conductivity of the coating were also neglected such as the temperature dependence of the thermal conductivity of air, radiative heat transport, convection in large pores and the heat transfer mechanism between hot gas and coating. Figure 7 shows the result of the present investigation in relation with results from literature, where the OOF algorithm has been applied on EB-PVD [20] and plasma sprayed [22] TBCs. These results are in good accordance proving an intrinsic correlation between the apparent porosity from a binary image and the calculated thermal conductivity independent on the type of coating. Yet, the discrepancy between the OOF and the experimental results in this figure points out the problem of over- or underestimating the effective porosity by developing the binary image in the OOF approach. Apparently, in the case of plasma sprayed TBCs the effective porosity has been underestimated while the opposite was the case for the EB-PVD.

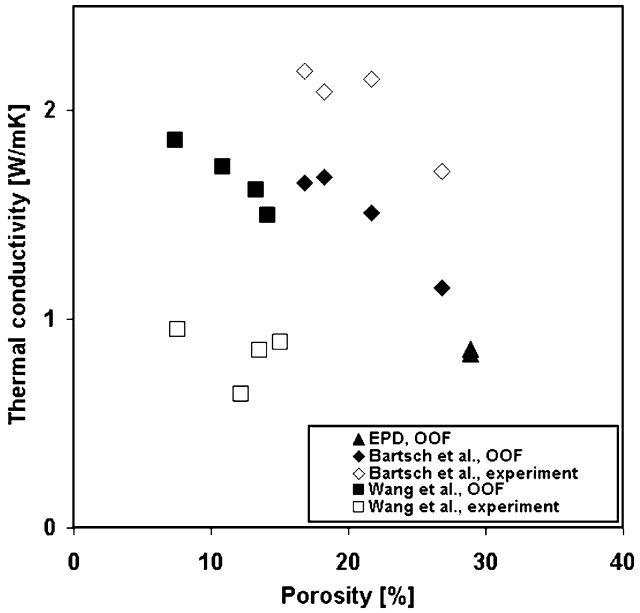

Fig. 7 Dependency of the room temperature thermal conductivity of as-coated TBCs on the coating porosity determined experimentally (empty symbols) and calculated from binary images using the OOF approach (filled symbols) for an EPD (triangle), EB-PVD (diamond) [20] and plasma sprayed (squares) [22] coatings

Conclusions

The deposition of a green zirconia layer on a dense steel substrate by EPD is characterised by a critical thickness, above which the coating will crack during drying. This critical thickness is a function of the curvature of the substrate. Depending on the curvature, a green thickness of 40–80 μm could be deposited, corresponding to a thickness of 15–30 μm in the sintered state. After sintering using a hybrid microwave technique, porous zirconia layers are obtained. These layers contained some iron, which is attributed to the penetration of a liquid iron layer formed on the surface of the substrate during microwave treatment. Depending on sintering temperature and time, an iron level of 1.5–3.7 wt% was measured.

By means of repeated deposition and microwave treatment, layers with a sintered thickness of 150–300 μm could be obtained. The microstructure of these layers is not homogeneous and contains large pores with a diameter of a few tens of μm. Values for the effective thermal conductivity of such layers were obtained applying object oriented finite element analysis. The values are comparable with those obtained for layers deposited by other techniques.

Acknowledgements This work was supported by the Research Fund K.U. Leuven within the project GOA/2005/08-TBA, the European Community's Human Potential Program under contract HPRN-CT-2002-00203, [SICMAC]. B. Baufeld acknowledges an individual Marie-Curie fellowship of the European Commission Nr. MEIF-CT-2005-010277.

References

1. DeMasi-Marcin JT, Gupta DK (1994) Surf Coat Tech 68/69:1
2. Zhang M, Heuer AH (2006) Scripta Mat 54:1265
3. Miller RA (1997) J Therm Spr Tech 6:35
4. Evans AG, Mumm DR, Hutchinson JW, Meier GH, Pettit FS (2001) Prog Mater Sci 46:505
5. Fritscher K, Schulz U, Peters M (2000) Proceedings of the 7th international symposium ceramic materials and compounds for engines, p. E121
6. Bruce RW (1998) Tribol Trans 41:399
7. Chen X, Wang R, Yao N, Evans AG, Hutchinson JW, Bruce RW (2003) Mater Sci Eng A 352:221

8. Borom MP, Johnson CA, Peluso LA (1996) Surf Coat Tech 86–87:116
9. Wortman DJ, Nagaraj BA, Duderstadt EC (1989) Mater Sci Eng A121:433
10. Meier SM, Gupta DK (1994) J Eng Gas Turbines Power Trans ASME 116:250
11. Goward GW (1998) Surf Coat Tech 108–109:73
12. Xu HB, Gong SK, Deng L (1998) Thin Solid Films 334:98
13. Stoever D, Funke C (1999) J Mater Process Technol 92–93:195
14. Van der Biest O, Vanderperre L (1999) Annu Rev Mater Sci 29:327
15. Put S, Vleugels J, Anne G, Van der Biest O (2003) Colloids Surf A: Physicochem Eng Aspects 222:223
16. Zhao C, Vleugels J, Groffils C, Luypaert PJ, Van Der Biest O (2000) Acta Materialia 48:3795
17. Hu MS, Thouless MD, Evans AG (1988) Acta Metallurgica 36:1301
18. Guo JJ, Lewis JA (1999) J Am Ceram Soc 82:2345
19. Fuller ERJ, Ruud JA, Hari NS, Grande JC, Mogro-Campero A (2002) Thermal property prediction via finite-element simulations, http://www.ctcms.nist.gov/%7Efuller/PRESENTATIONS/CocoaBeach_Thermal.pdf, as on 28 March 2006
20. Bartsch M, Fuller ERJ, Schulz U, Dorvaux JM, Lavigne O, Langer SA (2003) Ceram Eng Sci Proc (CESP) 24:549
21. Schulz U, Leyens C, Fritscher K, Peters M, Saruhan-Brings B, Lavigne O, Dorvaux J-M, Poulain M, Mevrel R, Caliez M (2003) Aerospace Sci Technol 7:73
22. Wang Z, Kulkarni A, Deshpande S, Nakamura T, Herman H (2003) Acta Mater 51:5319
23. Langer SA, Fuller ERJ, Carter WC (2001) Comput Sci Eng 3:1523
24. Zhu D, Miller RA (2000) J Therm Spr Tech 9:175
25. Dinwiddie RB, Beecher SC, Porter WD, Nagaraj BA (1996) Proceedings of the Turbo Expo '96, Birmingham UK. ASME
26. Rätzer-Scheibe HJ, Schulz U, Krell T (2006) Surf Coat Tech A200:5636